

Prediction and Comparative Analysis of Software Reliability Model Based on NHPP and Deep Learning

Youn Su Kim [†], Kwang Yoon Song [†] and In Hong Chang ^{*}

Department of Computer Science and Statistics, Chosun University, 309 Pilmun-daero, Dong-gu, Gwangju 61452, Republic of Korea; imk92315@naver.com (Y.S.K.); csssig@chosun.ac.kr (K.Y.S.)

^{*} Correspondence: ihchang@chosun.ac.kr

[†] These authors contributed equally to this work.

Abstract: Over time, software has become increasingly important in various fields. If the current software is more dependent than in the past and is broken owing to large and small issues, such as coding and system errors, it is expected to cause significant damage to the entire industry. To address this problem, the field of software reliability is crucial. In the past, efforts in software reliability were made to develop models by assuming a nonhomogeneous Poisson-process model (NHPP); however, as models became more complex, there were many special cases in which models fit well. Hence, this study proposes a software reliability model using deep learning that relies on data rather than mathematical and statistical assumptions. A software reliability model based on recurrent neural networks (RNN), long short-term memory (LSTM), and gated recurrent units (GRU), which are the most basic deep and recurrent neural networks, was constructed. The dataset was divided into two, Datasets 1 and 2, which both used 80% and 90% of the entire data, respectively. Using 11 criteria, the estimated and learned results based on these datasets proved that the software reliability model using deep learning has excellent capabilities. The software reliability model using GRU showed the most satisfactory results.

Keywords: software reliability model; deep learning; recurrent neural network; long short-term memory; gated recurrent unit



Citation: Kim, Y.S.; Song, K.Y.; Chang, I.H. Prediction and Comparative Analysis of Software Reliability Model Based on NHPP and Deep Learning. *Appl. Sci.* **2023**, *13*, 6730. <https://doi.org/10.3390/app13116730>

Academic Editor: Paolino Di Felice

Received: 20 April 2023

Revised: 25 May 2023

Accepted: 28 May 2023

Published: 31 May 2023



Copyright: © 2023 by the authors. Licensee MDPI, Basel, Switzerland. This article is an open access article distributed under the terms and conditions of the Creative Commons Attribution (CC BY) license (<https://creativecommons.org/licenses/by/4.0/>).

1. Introduction

Over time, software has become increasingly important in various fields. In the past, software helped with simple tasks or small parts in each industry; however, it has now been developed into a form that can perform basic roles in all-inclusive roles. If the current software is more dependent than in the past and is broken owing to large and small issues, such as certain coding and system errors, it is expected to cause significant damage to the entire industry. To address this problem, studies on software reliability, which measure how effectively the software works, are constantly being conducted. Software reliability tests the ability of software to not fail for a specified period and indicates how long the software can be used without failure.

Studies on software reliability have been conducted based on the software reliability model, assuming the Markov model and the non-homogeneous Poisson process (NHPP) [1]. However, since software failures follow a Poisson distribution, most related studies have been conducted based on the software reliability model, assuming NHPP. Previous studies on software reliability began when a software reliability model based on NHPP was developed by Goel and Okumoto [2]. It was assumed that software failures occur independently and do not affect each other. Subsequently, a study was conducted on an S-shaped curve model in which the number of cumulative software failures increased along the S curve [3–5]. In addition, a software reliability model study, assuming incomplete debugging in which the defects found in the test phase were not corrected or removed, was also conducted [6]. By

expanding on this, a study on a generalized incomplete debugging defect detection rate model was conducted [7–11]. The defect detection rate of each proposed model is in the form of a function. In addition, since the operating environment is different for each software, it is difficult to compare them equally. Thus, the software reliability model has been studied, considering uncertain factors in the operating environment [12,13].

As software develops over time, it becomes composed of complex and intertwined structures; therefore, studies on software reliability models are being conducted, assuming that software failures occur independently [14]. A software reliability model that assumes that previous errors will continuously affect software failures if they are not well fixed has been proposed, and a dependent software reliability model that assumes an uncertain operating environment has been studied [15,16].

As research progressed, several software reliability models studied under independent and dependent assumptions developed numerous models suitable for special cases, and generalizing them has been difficult. To address this, studies on software reliability models using deep learning, which is a nonparametric method, have been performed. Among the nonparametric software reliability models using deep learning, a study on software reliability models using deep neural networks was conducted [17], and a software reliability model using deep learning that applies failure data generated through open-source software was also proposed [18]. In addition, since software failure is a sequential data characteristic, the software reliability model using the recurrent neural network (RNN) and the long short-term memory (LSTM) was studied using this characteristic [19–21].

The software reliability model developed by NHPP has the problem that it fits well only in special cases because it adds special mathematical assumptions. Therefore, in this study, to solve this problem, we aim at the software reliability model utilizing deep learning among machine learning methods, which is a form that relies on given failure data. Since it is a data-dependent model, it is possible to develop a generalized software reliability model that considers all failures that occur in software without relying on special cases of software failures. In addition, in the past, software reliability models utilizing deep learning have been analyzed by applying methods, but in this study, we propose to add a deeper hidden layer of deep neural networks to the recurrent neural network series. If we develop a model that utilizes 100% of the data, it may cause an overfitting problem that only fits the trained data well. As a result, we also present the results for 80% and 90% of the data sets and the resulting predictions to prove superiority using 11 criteria comparisons. Section 2 presents the theoretical background of software reliability and deep learning. Section 3 introduces numerical examples, and finally, Section 4 presents the conclusions.

2. Software Reliability Model

2.1. Generalized Software Reliability Model

Software reliability refers to the probability that the software does not cause system failure for a certain period of time under specific conditions. The reliability function used to evaluate this is

$$R(t) = P(T > t) = \int_t^{\infty} f(u)du. \quad (1)$$

This indicates the probability of an operation over time t . The pdf $f(t)$ assumes the failure time or lifetime of the software to be a random variable T . We obtained the reliability function by assuming a distribution for the calculation. It was assumed that it follows an exponential distribution with parameter λ . Subsequently, we approach λ as an NHPP and propose a model in which λ is not a single constant value but a mean value function $m(t)$ that changes over time [1]. $N(t)$ is the number of failures up to time t and is a Poisson probability density function with parameter $m(t)$.

$$P\{N(t) = n\} = \frac{\{m(t)\}^n}{n!} e^{-m(t)}, n = 0, 1, 2, \dots, t \geq 0 \quad (2)$$

$m(t)$ is the integral of $\lambda(t)$, which is a strength function representing the number of instantaneous failures at time t and the mean value function from 0 to time t .

$$m(t) = \int_0^t \lambda(s)ds \tag{3}$$

The $m(t)$ is calculated using the relationship between the number of failures $a(t)$ at each time point and the failure detection rate $b(t)$.

$$\frac{dm(t)}{dt} = b(t)[a(t) - m(t)] \tag{4}$$

The software reliability model is developed using a differential equation, which is the basic form of the above equation. The software reliability model obtained by multiplying η in Equation (4) assumes an uncertain operating environment. Here, η is a parameter for the uncertainty of the operating environment, and N is the expected number of faults that exist in the software before testing [12].

$$\frac{dm(t)}{dt} = \eta b(t)[N - m(t)] \tag{5}$$

In addition, if $m(t)$ is multiplied again in Equation (4), a software reliability model can be derived assuming dependent failures, in which software failures at the previous time point affect failures at the next time point [14]. This is expressed in the following equation:

$$\frac{dm(t)}{dt} = b(t)[a(t) - m(t)]m(t) \tag{6}$$

If each differential equation is arranged in terms of $m(t)$ according to the conditions in Equations (4)–(6), a software reliability model that satisfies each condition can be derived. The developed software model is presented in Table 1. Models 1 to 6 are software reliability models obtained through the most basic form of differential equations; models 7 and 8 are those assuming uncertain operating environments; model 9 assumes dependent failures; and model 10 assumes the occurrence of dependent failures in an uncertain operating environment.

Table 1. NHPP software reliability models.

No.	Model	Mean Value Function	Note
1	Goel-Okumoto (GO) [2]	$m(t) = a(1 - e^{-bt})$	Concave
2	Yamada et al. (DS) [3]	$m(t) = a(1 - (1 + bt)e^{-bt})$	S-shape
3	Yamada et al. (YID) [6]	$m(t) = a(1 - e^{-bt})(1 - \frac{a}{b}) + \alpha at$	Concave
4	Pham-Zhang (PZ) [7]	$m(t) = \frac{((c+a)[1 - e^{-bt}] - [\frac{ab}{b-a}](e^{-at} - e^{-bt}))}{1 + \beta e^{-bt}}$	Both
5	Pham et al. (PNZ) [8]	$m(t) = \frac{a(1 - e^{-bt})(1 - \frac{a}{b}) + \alpha at}{1 + \beta e^{-bt}}$	Both
6	Teng-Pham (TP) [9]	$m(t) = \frac{a}{p-q} \left[1 - \left(\frac{\beta}{\beta + (p-q) \ln(\frac{c+bt}{c+1})} \right)^\alpha \right]$	S-shape
7	Chang et al. (TC) [12]	$m(t) = N \left[1 - \left(\frac{\beta}{\beta + (at)^b} \right)^\alpha \right]$	Both
8	Pham (Vtub) [13]	$m(t) = N \left[1 - \left(\frac{\beta}{\beta + a^{bt} - 1} \right)^\alpha \right]$	S-shape
9	Kim et al. (DPF) [15]	$m(t) = \frac{a}{1 + \frac{a}{h} \left(\frac{1+c}{c+e^{bt}} \right)^d}$	S-shape, Dependent

Table 1. *Cont.*

No.	Model	Mean Value Function	Note
10	Lee et al. (UDPF) [16]	$m(t) = N\left[1 - \left(\frac{\beta}{\alpha + bt - \ln(bt+1)}\right)^\alpha\right]$	S-shape Dependent

2.2. Software Reliability Model Using Deep Learning

2.2.1. Deep Neural Network

An artificial neural network is based on the biological structure of the human brain and consists of nonlinear neurons. Based on the information received by the five senses, humans think and judge last, as information moves from one neuron to the next. The neurons (nodes) present in each layer of an artificial neural network are the most basic information-processing units. The network structure consists of three layers: input, output, and hidden layers. The input layer plays the same role as the information obtained by human beings through their five senses or thoughts, whereas the output layer refers to thoughts or judgments based on this. Conversely, the hidden layer learns to think or judge while receiving signals from the previous layer and passes them to the next layer through an activation function. A deep neural network (DNN) refers to a form in which the number of hidden layers is large in an artificial neural network [22,23]. When data is inputted from the input layer, the next hidden layer moves to the next layer through an activation function after combining the input value, weight, and bias and is transmitted to the output layer. Equation (7) expresses the passing from each layer. It consists of the product of the transformed z value (input value) in the previous layer, the weight, and the sum of the biases.

$$u_{ij} = b_i + \sum_{k=1}^j W_{i,k} z_{i-1,k} \tag{7}$$

$$z_{ij} = f(u_{ij})$$

For each layer, the activation function when moving to the next layer mainly uses the sigmoid, hyperbolic tangent, and ReLU functions. As the activation function used when outputting the result passed to the last output layer is a continuous variable, an identity function was used.

The final predicted value was obtained using the above process. The difference between the predicted value y and the actual value t is calculated as a loss function. To minimize the difference between these values, the function is updated to have the minimum value based on the differential value for each weight and bias.

$$Loss = \sum_{i=1}^n (y_i - t_i)^2 \tag{8}$$

The weight update implies that the loss function is updated by the learning rate (α) based on the partial derivative value for a specific weight using the backpropagation algorithm. The deep neural network learns through a series of processes and outputs a predicted value that approximates the actual value.

$$W_{t+1} = W_t - \alpha \frac{\partial}{\partial W} Loss(W) \tag{9}$$

2.2.2. Recurrent Neural Network

The recurrent neural network is a model specialized for sequential data structures. It has cells that can remember the information of a previous point in the hidden layer of the most basic deep neural network. Therefore, it is suitable for time-series data because it is

designed to remember information from the past and influence future events. Figure 1a shows an image of the RNN model, and the formula is shown in Equation (10) [24].

$$h_t = \tanh(W_h h_{t-1} + W_x x_t + b) \tag{10}$$

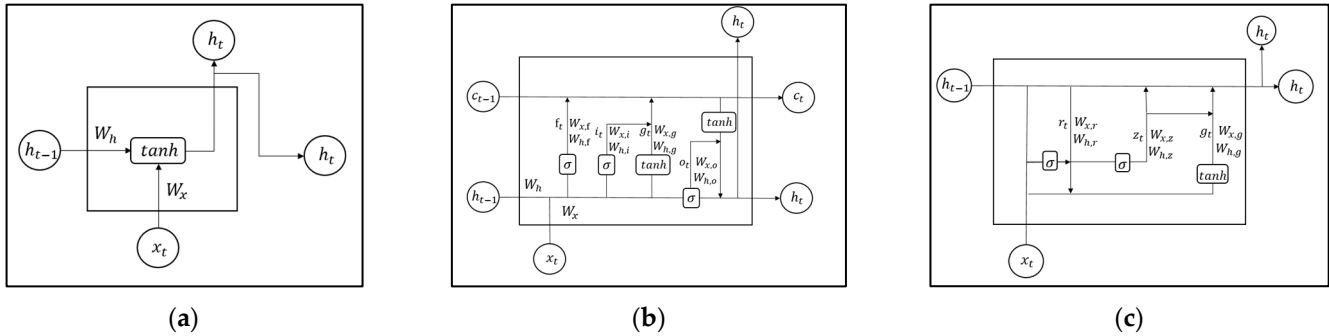


Figure 1. (a) Structure of RNN model; (b) Structure of LSTM model; (c) Structure of GRU model.

Its network structure reflects past time; however, it has a vanishing gradient problem that prevents it from accurately reflecting the information about the time that existed a long time ago as the time point becomes longer [25]. To address this problem, LSTM, which has a structure that can learn long-term dependence, was built. It contains the same hidden layer as the RNN structure; however, its internal structure differs. In LSTM, a memory cell c exists. This cell has a forget gate that determines how much previous information is reflected, an input gate that includes new information g , which indicates how much new information is reflected, and an output gate that indicates how much previous information is transferred to the next layer. The activation functions used at this time were the sigmoid function and the hyperbolic tangent. Information about the past is delivered by passing through three gates and memory cells. Through this, the gradient loss problem can be solved. Each gate follows Equation (11). Figure 1b shows the LSTM model [26].

$$\begin{aligned} f_t &= \sigma(x_t W_{x,f} + h_{t-1} W_{h,f} + b_f) \\ g_t &= \tanh(x_t W_{x,g} + h_{t-1} W_{h,g} + b_g) \\ i_t &= \sigma(x_t W_{x,i} + h_{t-1} W_{h,i} + b_i) \\ o_t &= \sigma(x_t W_{x,o} + h_{t-1} W_{h,o} + b_o) \\ c_t &= f_t \circ c_{t-1} + g_t \circ i_t \\ h_t &= o_t \circ \tanh(c_t) \end{aligned} \tag{11}$$

LSTM can solve the gradient loss problem in RNN; however, when going to the next step, LSTM goes through four operation processes if only one operation is performed. Processing big data may be inefficient because the number of computations increases fourfold. Complementing this, the gated recurrent unit (GRU) transmits a value to the next layer through three calculation processes in one layer. The GRU integrates the forget and input gates in the LSTM to create an update gate. In addition, it replaces the output gate with a reset gate, which determines the amount of previous information to be forgotten. The update gate determines how long the previous information should be kept. Through

Equation (12), the network learns while transferring to the next layer. Figure 1c shows an image of the GRU model [27].

$$\begin{aligned}
 r_t &= \sigma(x_t W_{x,r} + h_{t-1} W_{h,r} + b_r) \\
 z_t &= \sigma(x_t W_{x,z} + h_{t-1} W_{h,z} + b_z) \\
 g_t &= \tanh(x_t W_{x,g} + (r_t \circ h_{t-1}) W_{h,g} + b_g) \\
 h_t &= (1 - z_t) \circ g_t + z_t \circ h_{t-1}
 \end{aligned} \tag{12}$$

The software reliability model proposed in this study adds a deep neural network layer to add training depth to the predicted model, which reflects the past viewpoint through the hidden layer of the recurrent neural network. It proposes a learning model that goes through a deeper hidden layer to reflect the results of the past rather than just reflecting the past time of RNN series. This allows us to propose a software reliability model that can be generalized by solving problems that are only well suited to special cases of previously developed software reliability models. Among the software reliability models using deep learning, DNNs have three hidden layers, and RNNs have two. The number of nodes in the hidden layer was configured as the number of data points. Based on the given data, the number of nodes in the model should be limited to the number of data points to avoid estimating too many parameters compared to the data. The parameter optimization method used in the software reliability model using deep learning is Adam. Adam is a deep learning optimization method that combines the momentum method, which uses the acceleration of previous training, and the RMSprop method, which has a structure where the learning rate changes with each training instead of being constant. The formula is as follows:

$$\begin{aligned}
 u_{t+1} &= \beta_1 u_t + (1 - \beta_1) \left(\frac{\partial \text{Loss}(W)}{\partial W} \right), s_{t+1} = \beta_2 s_t + (1 - \beta_2) \left(\frac{\partial \text{Loss}(W)}{\partial W} \right)^2 \\
 W_{t+1} &= W_t - \alpha \frac{\hat{u}_t}{\sqrt{\hat{s}_t + \epsilon}}
 \end{aligned}$$

Let β_1 and β_2 be an exponential moving average of momentum and RMSprop. After obtaining the parameters u and s of momentum and RMSprop, update the weights by the learning rate α . In this study, to optimize the hyper-parameters, we set a range of hyper-parameters and iterated to find the optimal results. We want to find the optimal value by increasing the learning rate α by 5-times units from 0.0000001 to 0.01, and utilizing β_1 and β_2 of 0.9 and 0.99, respectively. Figure 2 shows the software reliability model that combines recurrent neural network types and deep neural networks among software reliability models using deep learning.

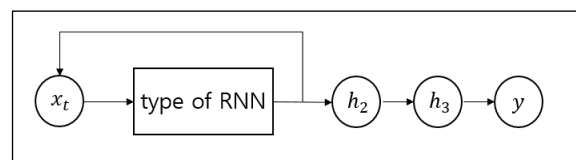


Figure 2. Software reliability model combining DNNs and type of RNN.

3. Numerical Example

3.1. Data Information

The dataset used in this study is the software failure data from PLC4X (<https://plc4x.apache.org>, accessed on 7 February 2022) and Apache Camel (<http://camel.apache.org>, accessed on 7 February 2022). Dataset 1 is from PLC4X, which is a set of libraries for communicating with industrial programmable logic controllers (PLCs) using a variety of protocols with a shared API. The data represent the cumulative number of failures occurring between December 2017 and January 2022. Dataset 2 is from Apache Camel,

which is an open-source integration framework that empowers you to quickly and easily integrate various systems consuming or producing data. Dataset 2 presents the cumulative number of failures between April 2011 and January 2022. Tables A1 and A2 show datasets 1 and 2. The software uses the Apache IoTDB (Database for the Internet of Things), which is a native IoT database with high performance for data management and analysis, deployable on the edge and in the cloud. Errors, such as bugs, code modifications, and database management errors, were recorded. It records defects and failures caused by bugs, new features, improvements, and tasks while operating the Apache IoTDB and is intended to estimate and predict software reliability models. Both datasets 1 and 2 used 80% and 90% of the entire data, which were utilized as training data necessary for training and parameter estimation, respectively. The remaining 20% and 10% of the data were used to compare predictions by substituting them for the training and estimated models.

3.2. Criteria

The software reliability models utilizing NHPP and deep learning were compared using 11 criteria based on the difference between the actual and predicted values. The mean squared error (MSE) and mean absolute error (MAE) were defined as the sum of the squared distances and absolute values of the distances between the estimated and actual values, divided by the difference between the number of observations and parameters [28,29].

$$\text{MSE} = \frac{\sum_{i=1}^n (\hat{m}(t_i) - y_i)^2}{n - m}, \text{MAE} = \frac{\sum_{i=1}^n |\hat{m}(t_i) - y_i|}{n - m} \quad (13)$$

The predictive ratio risk (PRR) was defined by dividing the distance between the actual and predicted values by the predicted value, and the predictive power (PP) was defined by dividing the distance between the actual and predicted values by the actual value [30].

$$\text{PRR} = \sum_{i=1}^n \left(\frac{\hat{m}(t_i) - y_i}{\hat{m}(t_i)} \right)^2, \text{PP} = \sum_{i=1}^n \left(\frac{\hat{m}(t_i) - y_i}{y_i} \right)^2 \quad (14)$$

R^2 is the coefficient of determination of the regression equation and determines the explanatory power by considering the number of parameters [31].

$$R^2 = 1 - \frac{\sum_{i=1}^n (\hat{m}(t_i) - y_i)^2}{\sum_{i=1}^n (y_i - \bar{y})^2} \quad (15)$$

The predicted relative variation (PRV) is the standard deviation of the prediction bias, where the bias is $\sum_{i=1}^n \left[\frac{\hat{m}(t_i) - y_i}{n} \right]$ and defined as [32]:

$$\text{PRV} = \sqrt{\frac{\sum_{i=1}^n (y_i - \hat{m}(t_i) - \text{Bias})^2}{n - 1}} \quad (16)$$

The root mean square prediction error (RMSPE) estimates the closeness with which the model predicts the observations [32]:

$$\text{RMSPE} = \sqrt{\text{Variance}^2 + \text{Bias}^2} \quad (17)$$

The mean error of prediction (MEOP) sums the absolute value of the deviation between the actual data and the estimated curve and is defined as [29]:

$$\text{MEOP} = \frac{\sum_{i=1}^n |\hat{m}(t_i) - y_i|}{n - m + 1} \quad (18)$$

The Theil statistic (TS) is the average percentage of deviation over all periods with respect to the actual values. This is defined as follows [29]:

$$TS = 100 * \sqrt{\frac{\sum_{i=1}^n (y_i - \hat{m}(t_i))^2}{\sum_{i=1}^n y_i^2}} \% \tag{19}$$

This criterion increases the penalty when a parameter is added to the model for a small sample [33].

$$PC = \left(\frac{n - m}{2}\right) \log\left(\frac{\sum_{i=1}^n (\hat{m}(t_i) - y_i)^2}{n}\right) + m\left(\frac{n - 1}{n - m}\right) \tag{20}$$

The preSSE (predicted sum squared error) refers to the sum of the differences between the predicted result value and the actual value, and the degree of estimation can be identified [34].

$$preSSE = \sum_{i=k+1}^n (\hat{m}(t_i) - y_i)^2 \tag{21}$$

Based on the above criteria, we compared the software reliability model utilizing NHPP with that using deep learning. For the same comparison, the number of criterion parameters affected by the number of parameters was set to zero. The closer R² is to 1, the better the result, and the closer it is to 0 for the other 10 criteria, the better the result. The goodness of the model fit was compared by calculating the criteria using R and MATLAB R2018b.

3.3. Results

3.3.1. Results of Dataset 1

Using Dataset 1, Table 2 shows the results of the parameter estimation of the software reliability model assuming NHPP and the structure of the software reliability model using deep learning. In addition, Dataset 1 was divided into 80% and 90%, and parameter estimation and model fitting were performed on the divided dataset. The structure of the software reliability model using deep learning consisted of three hidden layers, and the number of nodes in each layer was set according to the size of the training dataset. For the software reliability model of the recurrent neural network type, two deep neural networks were added, except for the recurrent neural network hidden layer. Here, Adam was used as the optimization method. The learning rate was set to 0.005 for the DNN and 0.0001 for the RNN, LSTM, and GRU.

Table 2. Parameter estimation and structure of model using Dataset 1.

No.	Model	80%	90%
1	GO	$\hat{a} = 1961.771, \hat{b} = 0.00065$	$\hat{a} = 8717.730, \hat{b} = 0.00015$
2	DS	$\hat{a} = 193.233, \hat{b} = 0.02730$	$\hat{a} = 160.532, \hat{b} = 0.03091$
3	YID	$\hat{a} = 97.401, \hat{b} = 0.00523, \hat{\alpha} = 0.10686$	$\hat{a} = 6.2301, \hat{b} = 0.05319, \hat{\alpha} = 0.34770$
4	PZ	$\hat{a} = 431.141, \hat{b} = 0.04005, \hat{\alpha} = 16.359, \hat{\beta} = 27.421, \hat{c} = 57.233$	$\hat{a} = 88.620, \hat{b} = 0.07843, \hat{\alpha} = 9.0099, \hat{\beta} = 12.248, \hat{c} = 2.0246$
5	PNZ	$\hat{a} = 69.646, \hat{b} = 0.01607, \hat{\alpha} = 0.07992, \hat{\beta} = 1.0343$	$\hat{a} = 71.272, \hat{b} = 0.08070, \hat{\alpha} = 0.00541, \hat{\beta} = 10.183$
6	TP	$\hat{a} = 72.610, \hat{b} = 0.06011, \hat{\alpha} = 1.8769, \hat{\beta} = 0.91909, \hat{c} = 13.7277, \hat{p} = 0.46681, \hat{q} = 0.09829$	$\hat{a} = 177.307, \hat{b} = 0.08976, \hat{\alpha} = 0.90527, \hat{\beta} = 3.2480, \hat{c} = 7.5811, \hat{p} = 1.5258, \hat{q} = 0.62709$

Table 2. Cont.

No.	Model	80%	90%
7	TC	$\hat{a} = 0.01628, \hat{b} = 1.5465, \hat{\alpha} = 1.1396,$ $\hat{\beta} = 16.708, \hat{N} = 1713.568$	$\hat{a} = 0.02299, \hat{b} = 1.5946, \hat{\alpha} = 4.9402,$ $\hat{\beta} = 15.240, \hat{N} = 233.487$
8	Vtub	$\hat{a} = 1.0018, \hat{b} = 1.4119, \hat{\alpha} = 0.18384,$ $\hat{\beta} = 9.0775, \hat{N} = 7788.528$	$\hat{a} = 1.1086, \hat{b} = 1.7068, \hat{\alpha} = 0.00730,$ $\hat{\beta} = 0.36680, \hat{N} = 165.881$
9	DPF	$\hat{a} = 80.628, \hat{b} = 0.00182,$ $\hat{c} = 0.41977, \hat{h} = 3.1673$	$\hat{a} = 76.498, \hat{b} = 0.00172,$ $\hat{c} = 0.23803, \hat{h} = 3.0477$
10	UDPF	$\hat{b} = 1.3315, \hat{\alpha} = 39.915,$ $\hat{\beta} = 5.4535, \hat{N} = 729.519$	$\hat{b} = 0.10265, \hat{\alpha} = 2.7233,$ $\hat{\beta} = 2.2206, \hat{N} = 257.005$
11	DNN	$\alpha = 0.005, \text{hidden layers} = 3, \text{optimizer} = \text{Adam}, \text{epoch} = 200$	
12	RNN	$\alpha = 0.0001, \text{hidden layers} = 2, \text{optimizer} = \text{Adam}, \text{epoch} = 200$	
13	LSTM	$\alpha = 0.0001, \text{hidden layers} = 2, \text{optimizer} = \text{Adam}, \text{epoch} = 200$	
14	GRU	$\alpha = 0.0001, \text{hidden layers} = 2, \text{optimizer} = \text{Adam}, \text{epoch} = 200$	

Table 3 lists the result values of the criteria using 80% of Dataset 1. The values for MSE, PRV, RMSPE, TS, and PC in LSTM were the lowest at 2.0069, 0.1345, 1.4168, 4.9250, and 14.5574, respectively. GRU showed the lowest values of 0.6706 and 1.1032 in PRR and PP, and the lowest values of MAE and MEOP of 1.21164 and 1.186 were observed in UDPF, respectively. The R^2 value was the highest for LSTM and GRU at 0.9929. In LSTM, 6 out of 10 criteria showed good results. For the predictions of 10% and 20%, the DPF model with a preSSE value of 47.645 had the lowest result among the software reliability models assuming NHPP. In contrast, most software reliability models using deep learning showed values in the 20-point range, and the LSTM model showed the smallest value of 21.570.

Table 3. Comparison of all criteria using 80% of Dataset 1.

No.	Model	MSE	MAE	PRR	PP	R^2	PRV	RMSPE	MEOP	TS	PC	preSSE
1	GO	21.1902	4.0601	4.7030	11.9204	0.9254	4.2944	4.6544	3.9586	16.0037	60.5184	768.422
2	DS	3.9990	1.6435	1853.84	3.9028	0.9859	1.9503	2.0240	1.6024	6.9523	28.0021	64.894
3	YID	2.7404	1.2988	26.5655	2.4337	0.9904	1.6685	1.6768	1.2663	5.7552	20.6324	454.284
4	PZ	2.8043	1.2790	15.2300	2.6449	0.9901	1.6951	1.6965	1.2471	5.8219	21.0819	8306.771
5	PNZ	2.7172	1.2864	22.5012	2.4253	0.9904	1.6634	1.6698	1.2543	5.7308	20.4666	150,716.8
6	TP	2.7168	1.2888	18.3855	2.3926	0.9904	1.6648	1.6697	1.2566	5.7303	20.4634	7839.272
7	TC	3.1185	1.4057	221.7352	3.0482	0.9890	1.7648	1.7884	1.3705	6.1394	23.1529	224.970
8	Vtub	2.8788	1.3403	108.599	2.8416	0.9899	1.6990	1.7184	1.3068	5.8987	21.5931	455.315
9	DPF	3.1625	1.3642	0.9386	1.9608	0.9889	1.7976	1.8015	1.3301	6.1826	23.4260	47.645
10	UDPF	2.5427	1.2164	0.8600	1.2500	0.9911	1.6154	1.6154	1.1860	5.5437	19.1722	876.104
11	DNN	2.4373	1.4791	0.7005	1.1789	0.9914	0.5061	1.5633	1.4421	5.4275	18.3463	25.294
12	RNN	2.1147	1.4127	0.7380	1.2844	0.9926	0.3495	1.4553	1.3774	5.0557	15.5784	22.274
13	LSTM	2.0069	1.4104	0.8014	1.4432	0.9929	0.1345	1.4168	1.3751	4.9250	14.5574	21.570
14	GRU	2.0159	1.3983	0.6706	1.1032	0.9929	0.2493	1.4204	1.3634	4.9362	14.6454	23.872

Table 4 lists the result values of the criteria using 90% of Dataset 1. MSE, RMSPE, TS, and PC were the lowest in GRU at 1.9961, 0.9948, 1.413, 4.1991, and 16.1831, respectively, and PRV was the smallest in LSTM at 0.1251. In addition, PRR and PP in UDPF showed the lowest values of 0.6386 and 0.9113, and MAE and MEOP were 1.3714 and 1.3409 in DPF, respectively. The R^2 value was the largest at 0.9948. In GRU, 5 out of 10 criteria showed good results. In preSSE, the TC, DS, and Vtub models showed very small values of 6.367, 6.537, and 7.340, respectively. In the software reliability model using deep learning, RNN showed the smallest value of 11.397, followed by LSTM at 11.755. The resulting values showed good results for the software reliability model, assuming NHPP.

Table 4. Comparison of all criteria using 90% of Dataset 1.

No.	Model	MSE	MAE	PRR	PP	R ²	PRV	RMSPE	MEOP	TS	PC	preSSE
1	GO	22.6581	4.3155	4.7797	13.4021	0.9407	4.4490	4.8071	4.2196	14.1477	69.6287	321.655
2	DS	3.9569	1.6600	1636.27	3.7881	0.9896	1.9677	2.0112	1.6231	5.9122	31.2376	6.537
3	YID	3.5588	1.5488	58.9754	2.7164	0.9907	1.9001	1.9081	1.5144	5.6069	28.9044	11.837
4	PZ	3.1010	1.4570	31.2349	2.4008	0.9919	1.7750	1.7812	1.4246	5.2339	25.8753	2395.537
5	PNZ	3.1296	1.4638	27.1085	2.3403	0.9918	1.7798	1.7893	1.4313	5.2580	26.0772	40.741
6	TP	3.2108	1.4898	26.6591	2.3619	0.9916	1.8069	1.8125	1.4567	5.3257	26.6407	4948.058
7	TC	3.6277	1.5687	262.6646	3.1326	0.9905	1.9117	1.9263	1.5338	5.6609	29.3263	6.367
8	Vtub	3.4308	1.5331	82.7369	2.6383	0.9910	1.8662	1.8735	1.4990	5.5051	28.0984	7.340
9	DPF	3.0682	1.3714	0.8756	1.7908	0.9920	1.7676	1.7718	1.3409	5.2061	25.6412	65.275
10	UDPF	2.9984	1.3889	0.6386	0.9113	0.9922	1.7515	1.7516	1.3581	5.1465	25.1349	1709.197
11	DNN	2.5868	1.5030	0.7327	1.3150	0.9932	0.5792	1.6107	1.4696	4.7803	21.8866	13.471
12	RNN	2.0731	1.4332	0.8317	1.5417	0.9946	0.1402	1.4400	1.4013	4.2794	17.0167	11.397
13	LSTM	2.0257	1.4179	0.7584	1.3192	0.9947	0.1251	1.4234	1.3864	4.2302	16.5077	11.755
14	GRU	1.9961	1.4061	0.7593	1.331	0.9948	0.1392	1.413	1.3749	4.1991	16.1831	12.103

3.3.2. Results of Dataset 2

Using Dataset 2, Table 5 shows the results of the parameter estimation of the software reliability model assuming NHPP and the structure of the software reliability model using deep learning. Similar to Dataset 1, Dataset 2 was divided into 80% and 90%, and parameter estimation and model fitting were performed on the divided dataset. The structure of the software reliability model using deep learning consists of three hidden layers, as in Dataset 1, and the number of nodes in each layer was set according to the size of the training dataset. The learning rates were set to 0.000001 for DNN and 0.00001 for RNN, LSTM, and GRU.

Table 5. Parameter estimation and structure of model using Dataset 2.

No.	Model	80%	90%
1	GO	$\hat{a} = 15383.72, \hat{b} = 0.00010$	$\hat{a} = 37605.84, \hat{b} = 0.00005$
2	DS	$\hat{a} = 13332.14, \hat{b} = 0.00182$	$\hat{a} = 53880.83, \hat{b} = 0.00091$
3	YID	$\hat{a} = 49.407, \hat{b} = 0.00121, \hat{\alpha} = 0.66627$	$\hat{a} = 10.855, \hat{b} = 0.00145, \hat{\alpha} = 2.7890$
4	PZ	$\hat{a} = 564.590, \hat{b} = 0.2938, \hat{\alpha} = 0.35523, \hat{\beta} = 31.536, \hat{c} = 0.04628$	$\hat{a} = 3566157.77, \hat{b} = 0.02095, \hat{\alpha} = 0.14865, \hat{\beta} = 119107.58, \hat{c} = 3567.64$
5	PNZ	$\hat{a} = 166.155, \hat{b} = 0.01033, \hat{\alpha} = 0.06270, \hat{\beta} = 4.2225$	$\hat{a} = 284.863, \hat{b} = 0.01104, \hat{\alpha} = 0.07397, \hat{\beta} = 11.590$
6	TP	$\hat{a} = 4.1953, \hat{b} = 0.08837, \hat{\alpha} = 7.3884, \hat{\beta} = 2.8696, \hat{c} = 1.6579, \hat{p} = 0.04236, \hat{q} = 0.10460$	$\hat{a} = 49.417, \hat{b} = 0.06702, \hat{\alpha} = 0.01198, \hat{\beta} = 0.02904, \hat{c} = 2.4430, \hat{p} = 0.20147, \hat{q} = 0.20537$
7	TC	$\hat{a} = 0.01344, \hat{b} = 1.9930, \hat{\alpha} = 0.00754, \hat{\beta} = 0.39594, \hat{N} = 2857.101$	$\hat{a} = 0.00307, \hat{b} = 2.22599, \hat{\alpha} = 4.7647, \hat{\beta} = 118.747, \hat{N} = 73382.23$
8	Vtub	$\hat{a} = 1.0005, \hat{b} = 2.2792, \hat{\alpha} = 0.00754, \hat{\beta} = 0.39594, \hat{N} = 1562.143$	$\hat{a} = 1.0128, \hat{b} = 1.1078, \hat{\alpha} = 16.018, \hat{\beta} = 1060.760, \hat{N} = 2049.573$
9	DPF	$\hat{a} = 322.915, \hat{b} = 0.00018, \hat{c} = 0.33127, \hat{h} = 6.4475$	$\hat{a} = 994.419, \hat{b} = 0.00005, \hat{c} = 0.57131, \hat{h} = 10.012$
10	UDPF	$\hat{b} = 652.600, \hat{\alpha} = 21497.41, \hat{\beta} = 8.9936, \hat{N} = 1804.06$	$\hat{b} = 13.526, \hat{\alpha} = 2439.458, \hat{\beta} = 10.564, \hat{N} = 192350.3$
11	DNN	$\alpha = 0.000001, \text{hidden layers} = 3, \text{optimizer} = \text{Adam}, \text{epoch} = 200$	
12	RNN	$\alpha = 0.00001, \text{hidden layers} = 2, \text{optimizer} = \text{Adam}, \text{epoch} = 200$	
13	LSTM	$\alpha = 0.00001, \text{hidden layers} = 2, \text{optimizer} = \text{Adam}, \text{epoch} = 200$	
14	GRU	$\alpha = 0.00001, \text{hidden layers} = 2, \text{optimizer} = \text{Adam}, \text{epoch} = 200$	

Table 6 shows the result values of the criteria using 80% of Dataset 2. The values of MSE, MAE, PRV, RMSPE, MEOP, TS, and PC in GRU were the lowest at 4.5494, 2.0688, 0.5218, 2.1336, 2.0489, 2.2311, and 79.0128, respectively, and R² of 0.9988 in GRU and LSTM appeared the highest. PRR showed the lowest value of 1.5342 in DNN, and PP showed the smallest value of 1.7716 in TP. In GRU, 8 out of 10 criteria showed good results. Among the software reliability models assuming NHPP, the model with the lowest result was the Vtub model, with a preSSE value of 159,551.23. In contrast, most software reliability models using deep learning showed smaller values than the existing software reliability models; among them, the RNN model showed the smallest value of 71.06.

Table 6. Comparison of all criteria using 80% of Dataset 2.

No.	Model	MSE	MAE	PRR	PP	R ²	PRV	RMSPE	MEOP	TS	PC	preSSE
1	GO	514.6996	20.0326	17.3582	100.887	0.8664	21.0794	22.7819	19.8400	23.7311	322.5348	735,386.2
2	DS	13.7076	3.0740	2256.700	8.8015	0.9964	3.6874	3.7202	3.0445	3.8728	135.8146	202,541.7
3	YID	12.1406	2.8671	215.3384	7.1101	0.9968	3.4643	3.5010	2.8395	3.6447	129.5631	184,160.8
4	PZ	10.0437	2.5378	3299.707	9.6331	0.9974	3.1828	3.1847	2.5134	3.3150	119.7981	174,920.2
5	PNZ	9.6155	2.4483	7.2913	1.9345	0.9975	3.1155	3.1160	2.4248	3.2436	117.5539	1,643,848
6	TP	11.0679	2.6448	5.4184	1.7716	0.9971	3.3366	3.3430	2.6194	3.4800	124.7987	2,037,721
7	TC	13.4688	3.0404	2453.543	9.2252	0.9965	3.6077	3.6872	3.0112	3.8389	134.9098	189,842.4
8	Vtub	10.7640	2.7480	5303.130	7.7007	0.9972	3.2707	3.2966	2.7216	3.4318	123.3649	159,551.2
9	DPF	16.6392	3.3789	5.4085	88.826	0.9957	4.0398	4.0985	3.3464	4.2668	145.7959	305,246.7
10	UDPF	22.5801	3.8694	99.4808	9.7126	0.9941	4.6880	4.7742	3.8322	4.9705	161.5192	274,796.2
11	DNN	5.8181	2.1792	1.5342	4.0310	0.9985	1.0391	2.4143	2.1583	2.5231	91.6808	355.63
12	RNN	4.8223	2.0739	2.1101	9.9452	0.9987	0.7255	2.1971	2.0539	2.2970	82.0123	71.06
13	LSTM	4.6712	2.0805	2.3802	16.1958	0.9988	0.5882	2.1621	2.0605	2.2608	80.3730	290.41
14	GRU	4.5494	2.0688	2.1001	9.9841	0.9988	0.5218	2.1336	2.0489	2.2311	79.0128	347.92

Table 7 shows the result values for the criteria using 90% of Dataset 2. MSE, PRV, RMSPE, TS, and PC showed the smallest values of 8.8655, 0.9189, 2.9787, 2.3336, and 1237.5573, respectively, in GRU, and R² showed the largest value of 0.9988 in the same model. MAE and MEOP had the smallest values of 2.8168 and 2.7928, respectively, in RNN. PRR was 1.6236 in DNN, and PP was the smallest at 1.4301 in Vtub. In GRU, 6 out of 10 criteria showed good results. Regarding the preSSE value, the GRU model showed the smallest value of 468.03 among the software reliability models using deep learning.

Table 7. Comparison of all criteria using 90% of Dataset 2.

No.	Model	MSE	MAE	PRR	PP	R ²	PRV	RMSPE	MEOP	TS	PC	preSSE
1	GO	1278.733	30.0077	23.6240	173.2001	0.8256	33.3020	35.8928	29.7512	28.0264	415.9016	426,981.8
2	DS	98.7794	7.0277	2204.006	8.9742	0.9865	9.8441	9.9807	6.9676	7.7895	267.3789	114,300.6
3	YID	97.1781	6.9453	840.7242	8.4733	0.9867	9.7596	9.8995	6.8859	7.7261	266.4310	113,140.1
4	PZ	27.9916	4.2381	677.6398	67.5837	0.9962	5.3037	5.3136	4.2019	4.1466	194.2418	26,776.2
5	PNZ	39.4936	4.7960	18.9956	3.8443	0.9946	6.2657	6.3113	4.7550	4.9254	214.2075	1,165,855
6	TP	13.6426	2.9286	4.0108	1.6448	0.9981	3.6944	3.7095	2.9035	2.8948	152.5569	1,390,597
7	TC	64.3763	6.6342	19,228.33	14.4663	0.9912	7.8678	8.0567	6.5775	6.2884	242.5466	65,012.80
8	Vtub	26.1124	3.8598	3.7169	1.4301	0.9964	5.1293	5.1322	3.8268	4.0050	190.2112	23,868.05
9	DPF	50.3622	6.2521	9.2044	251.4521	0.9931	7.0064	7.1264	6.1987	5.5620	228.3074	28,590.91
10	UDPF	36.7890	4.7296	4.2437	47.5652	0.9950	6.0896	6.0917	4.6891	4.7537	210.0929	33,114.75
11	DNN	11.4930	2.8455	1.6236	4.2855	0.9984	1.8509	3.3945	2.8211	2.6570	142.612	680.76
12	RNN	10.3925	2.8168	2.9032	22.1128	0.9986	1.5746	3.2271	2.7928	2.5266	136.7744	1122.65
13	LSTM	11.7785	2.8708	2.9508	40.5778	0.9984	1.8888	3.4365	2.8463	2.6898	144.0352	1251.45
14	GRU	8.8655	2.8335	2.8749	19.0924	0.9988	0.9189	2.9787	2.8092	2.3336	127.5573	468.03

Figures 3 and 4 are graphs that combine the estimated and trained values for 80% and 90% of the data above with the predicted values for the remaining 20% and 10%. The points

before the black line are estimated values, and the points after the black line are predicted values.

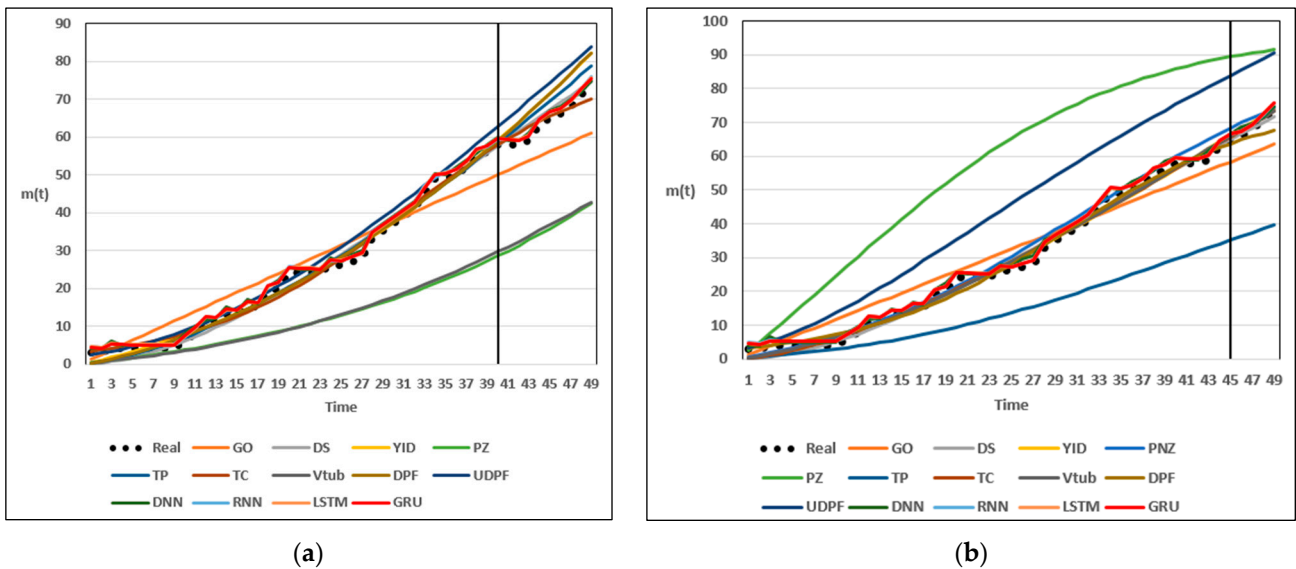


Figure 3. (a) Estimated and predicted value for 80% of Dataset 1; (b) Estimated and predicted value for 90% of Dataset 1.

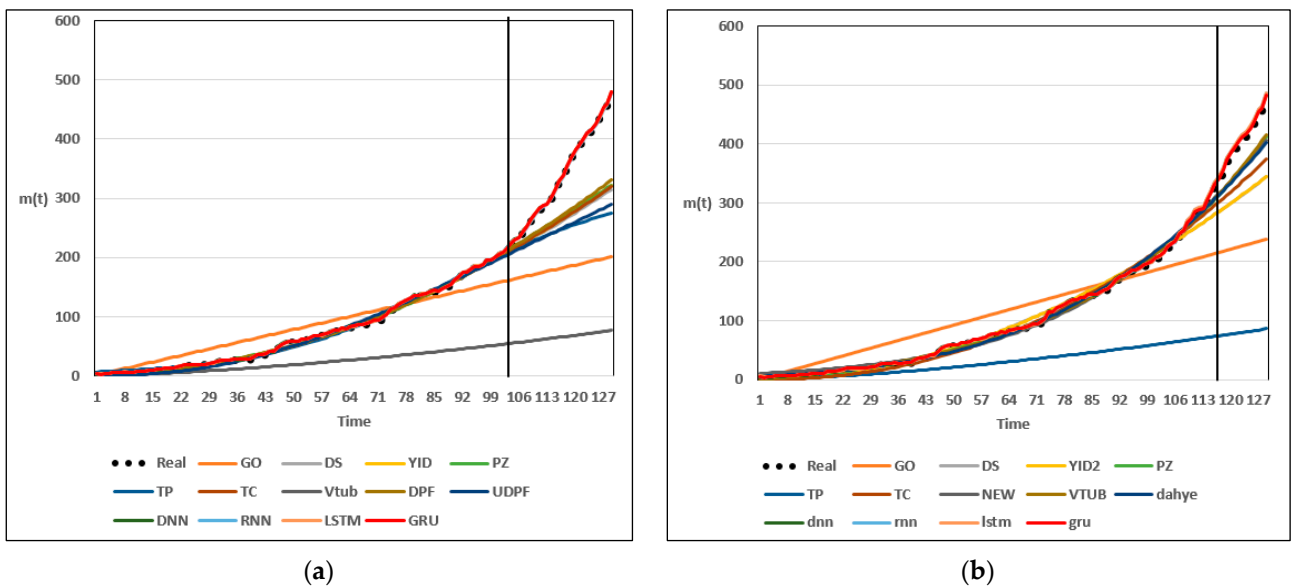


Figure 4. (a) Estimated and predicted value for 80% of Dataset 2; (b) Estimated and predicted value for 90% of Dataset 2.

3.4. Confidence Interval

In this study, GRU, the software reliability model that showed the best results among the proposed models, was used to obtain the confidence interval. In addition, the difference in the distribution between the predicted and actual data values of the other models was compared. The confidence interval follows Equation (22). Since software failures follow a Poisson distribution, we take the mean and variance as $\hat{m}(t)$. z_α is defined as the $100(1 - \alpha)/2$ percentile of the standard normal distribution [35]. A 95% confidence interval was used.

$$\hat{m}(t) + z_\alpha \sqrt{\hat{m}(t)} \tag{22}$$

Tables A3 and A4 show the predicted values and corresponding confidence intervals for the remaining 20% and 10% of the data based on the estimated and trained models for 80% and 90% of Dataset 1. The bolded values indicate that the actual data values do not fall within the prediction intervals. For 80% of Dataset 1, the other NHPP software reliability models, except for PNZ, PZ, and Vtub, and the software reliability models using deep learning, predicted well within the 95% confidence interval. For 90% of Dataset 1, the other NHPP software reliability models (except PNZ, PZ, TP, and UDPF) and the software reliability models using deep learning performed well within the 95% confidence interval.

Tables A5 and A6 show the predicted values and corresponding confidence intervals for the remaining 20% and 10% of the data based on the estimated and trained models for 80% and 90% of Dataset 2. For 80% of Dataset 2, the GO, PNZ, and TP models showed results where the actual data was not within the prediction confidence interval at all, while the DS model showed results where the actual data was within the 95% prediction confidence interval up to the 108th time, the YID, TC, DPF, and UDPF models up to the 109th time, and the PZ, Vtub model up to the 110th time. For 90% of Dataset 2, the NHPP software reliability models showed that the PZ, Vtub, DPF, and UDPF models resulted in the actual data falling within the 95% prediction confidence interval up to the 118th time. Except for the PZ, Vtub, DPF, and UDPF models, none of the NHPP software reliability models had the actual data fall within the predicted confidence interval. The software reliability models using deep learning performed well, with predictions within the 95% confidence interval. Except for the models that do not fall within the 95% confidence intervals shown in Tables A3–A6, the remaining models showed good results in following the data trend, and the software reliability models using deep learning showed good estimation and prediction results in following the data trend.

4. Conclusions

In this study, the software reliability models using NHPP and deep learning were compared. Regarding the software reliability model using deep learning, a model composed of deep neural networks and recurrent neural networks (RNN, LSTM, and GRU) that have been applied to time-series data characteristics was used. It was constructed by including the hidden layer of the neural network. Using Datasets 1 and 2, it was confirmed that this model showed better estimation and predictive power than existing software reliability models. Among them, the software reliability of the recurrent neural network series showed better results, and as a result of fitting with 80% and 90% datasets, the software reliability model with the deep neural network added to the GRU showed the best results. In addition, the software reliability model of the recurrent neural network showed good results when the predicted values were compared with the remaining datasets. The NHPP software reliability model showed results that relatively fit the data well with a small number of time points; however, it showed a significant increase as the number of time points increased. On the other hand, the software neural network using deep learning showed results that fit the data trend well, even when the time point was large.

However, software reliability models using deep learning always face the problem of overfitting. Therefore, to address this, we plan to conduct research on software reliability models based on mathematical and statistical assumptions by grafting them together with the NHPP software reliability models. Through this, we aim to create a stable, data-dependent, and complementary model with a more mathematical basis.

Author Contributions: Conceptualization, K.Y.S. and I.H.C.; funding acquisition, K.Y.S. and I.H.C.; software, Y.S.K.; writing—original draft, Y.S.K.; writing—review and editing, K.Y.S. and I.H.C. All authors have read and agreed to the published version of the manuscript.

Funding: This research was supported by the Basic Science Research Program through the National Research Foundation of Korea (NRF), funded by the Ministry of Education (NRF-2021R1F1A1048592, NRF-2021R1I1A1A01059842).

Institutional Review Board Statement: Not applicable.

Informed Consent Statement: Not applicable.

Data Availability Statement: Data is available in a publicly accessible repository.

Acknowledgments: This study was supported by the National Research Foundation of Korea (NRF).

Conflicts of Interest: The authors declare no conflict of interest.

Appendix A

Table A1. Cumulative number of software failures in Dataset 1.

Index	Failures	Cumulative Failures	Index	Failures	Cumulative Failures	Index	Failures	Cumulative Failures
1	3	3	18	4	19	35	0	49
2	0	3	19	1	20	36	1	50
3	1	4	20	4	24	37	2	52
4	0	4	21	0	24	38	3	55
5	0	4	22	0	24	39	1	56
6	0	4	23	0	24	40	2	58
7	0	4	24	2	26	41	0	58
8	0	4	25	0	26	42	0	58
9	0	4	26	1	27	43	1	59
10	2	6	27	1	28	44	4	63
11	2	8	28	5	33	45	2	65
12	3	11	29	2	35	46	1	66
13	0	11	30	2	37	47	2	68
14	2	13	31	2	39	48	3	71
15	0	13	32	2	41	49	3	74
16	2	15	33	4	45	50	2	76
17	0	15	34	4	49			

Table A2. Cumulative number of software failures in Dataset 2.

Index	Failures	Cumulative Failures									
1	1	1	34	0	25	67	0	85	100	3	197
2	0	1	35	1	26	68	1	86	101	6	203
3	1	2	36	0	26	69	2	88	102	3	206
4	0	2	37	0	26	70	3	91	103	6	212
5	2	4	38	1	27	71	1	92	104	9	221
6	0	4	39	0	27	72	3	95	105	6	227
7	0	4	40	3	30	73	6	101	106	3	230
8	1	5	41	3	33	74	9	110	107	12	242
9	0	5	42	1	34	75	2	112	108	6	248
10	0	5	43	2	36	76	6	118	109	13	261
11	1	6	44	3	39	77	3	121	110	8	269
12	0	6	45	0	39	78	4	125	111	10	279
13	0	6	46	6	45	79	4	129	112	5	284
14	2	8	47	5	50	80	4	133	113	3	287
15	0	8	48	4	54	81	0	133	114	11	298
16	1	9	49	2	56	82	3	136	115	15	313
17	0	9	50	1	57	83	1	137	116	12	325
18	2	11	51	0	57	84	4	141	117	10	335
19	1	12	52	3	60	85	1	142	118	15	350
20	0	12	53	1	61	86	0	142	119	16	366
21	1	13	54	1	62	87	3	145	120	12	378
22	2	15	55	3	65	88	4	149	121	8	386
23	2	17	56	1	66	89	3	152	122	12	398
24	0	17	57	1	67	90	6	158	123	8	406
25	0	17	58	2	69	91	7	165	124	6	412
26	0	17	59	3	72	92	6	171	125	10	422

Table A2. Cont.

Index	Failures	Cumulative Failures									
27	0	17	60	3	75	93	2	173	126	10	432
28	1	18	61	1	76	94	4	177	127	17	449
29	1	19	62	2	78	95	5	182	128	6	455
30	1	20	63	0	78	96	1	183	129	21	476
31	3	23	64	3	81	97	3	186	130	26	502
32	2	25	65	1	82	98	6	192			
33	0	25	66	3	85	99	2	194			

Table A3. 95% Prediction confidence interval of software reliability models from 80% of Dataset 1.

Time	Real	Prediction	GO Upper	Lower	Prediction	DS Upper	Lower	Prediction	YID Upper	Lower
40	58	49.98	63.84	36.13	57.58	72.46	42.71	59.04	74.10	43.98
41	58	51.22	65.24	37.19	59.51	74.63	44.39	61.44	76.80	46.07
42	58	52.45	66.64	38.26	61.44	76.80	46.08	63.88	79.54	48.21
43	59	53.68	68.04	39.32	63.36	78.96	47.76	66.36	82.33	50.39
44	63	54.91	69.44	40.39	65.27	81.10	49.43	68.88	85.15	52.62
45	65	56.14	70.83	41.46	67.17	83.23	51.11	71.45	88.01	54.88
46	66	57.37	72.22	42.53	69.06	85.35	52.77	74.05	90.92	57.19
47	68	58.60	73.60	43.60	70.94	87.45	54.43	76.70	93.86	59.53
48	71	59.83	74.99	44.67	72.81	89.54	56.09	79.38	96.85	61.92
49	74	61.05	76.37	45.74	74.67	91.61	57.73	82.11	99.87	64.35
Time	Real	Prediction	PNZ Upper	Lower	Prediction	PZ Upper	Lower	Prediction	TP Upper	Lower
40	58	163.96	189.05	138.86	28.51	38.97	18.04	58.28	73.24	43.31
41	58	168.86	194.33	143.39	29.87	40.58	19.16	60.47	75.71	45.23
42	58	173.80	199.64	147.96	31.28	42.24	20.31	62.69	78.21	47.17
43	59	178.77	204.97	152.56	32.73	43.94	21.52	64.93	80.72	49.13
44	63	183.77	210.34	157.20	34.24	45.70	22.77	67.19	83.26	51.13
45	65	188.81	215.74	161.88	35.79	47.52	24.06	69.48	85.81	53.14
46	66	193.88	221.17	166.59	37.40	49.38	25.41	71.78	88.39	55.18
47	68	198.98	226.63	171.33	39.05	51.30	26.80	74.11	90.99	57.24
48	71	204.12	232.12	176.11	40.76	53.28	28.25	76.46	93.60	59.32
49	74	209.28	237.64	180.93	42.53	55.31	29.75	78.83	96.24	61.43
Time	Real	Prediction	TC Upper	Lower	Prediction	Vtub Upper	Lower	Prediction	DPF Upper	Lower
40	58	57.84	72.75	42.94	29.64	40.31	18.97	58.94	73.98	43.89
41	58	59.53	74.65	44.40	31.00	41.91	20.08	61.33	76.68	45.98
42	58	61.13	76.45	45.80	32.38	43.54	21.23	63.78	79.43	48.13
43	59	62.64	78.15	47.13	33.80	45.19	22.40	66.28	82.23	50.32
44	63	64.07	79.76	48.38	35.23	46.87	23.60	68.82	85.08	52.56
45	65	65.42	81.27	49.57	36.69	48.57	24.82	71.41	87.97	54.85
46	66	66.68	82.68	50.67	38.18	50.29	26.07	74.05	90.92	57.19
47	68	67.86	84.00	51.71	39.68	52.02	27.33	76.75	93.92	59.57
48	71	68.95	85.23	52.68	41.20	53.78	28.62	79.49	96.96	62.01
49	74	69.97	86.36	53.57	42.74	55.55	29.92	82.28	100.06	64.50
Time	Real	Prediction	UDPF Upper	Lower	Prediction	DNN Upper	Lower	Prediction	RNN Upper	Lower
40	58	62.68	78.19	47.16	60.01	75.20	44.83	59.46	74.57	44.34
41	58	64.97	80.77	49.18	59.02	74.07	43.96	59.24	74.32	44.15
42	58	67.29	83.37	51.21	59.02	74.07	43.96	59.19	74.27	44.11
43	59	69.62	85.97	53.26	61.01	76.32	45.70	60.24	75.45	45.03
44	63	71.96	88.58	55.33	64.39	80.12	48.66	64.71	80.48	48.95

Table A3. *Cont.*

Time	Real	UDPF			DNN			RNN		
		Prediction	Upper	Lower	Prediction	Upper	Lower	Prediction	Upper	Lower
45	65	74.31	91.20	57.41	67.01	83.06	50.97	66.64	82.64	50.64
46	66	76.67	93.83	59.50	68.01	84.18	51.85	67.41	83.50	51.32
47	68	79.03	96.46	61.61	70.01	86.41	53.61	69.44	85.77	53.11
48	71	81.41	99.10	63.73	71.70	88.30	55.11	72.65	89.35	55.94
49	74	83.79	101.73	65.85	74.70	91.65	57.76	75.82	92.88	58.75
Time	Real	LSTM			GRU					
		Prediction	Upper	Lower	Prediction	Upper	Lower			
40	58	59.51	74.63	44.39	59.72	74.86	44.57			
41	58	59.42	74.53	44.31	59.27	74.36	44.18			
42	58	59.36	74.46	44.26	59.13	74.20	44.06			
43	59	60.33	75.55	45.10	60.26	75.47	45.04			
44	63	64.53	80.27	48.78	64.78	80.56	49.00			
45	65	66.53	82.52	50.55	66.78	82.80	50.77			
46	66	67.46	83.55	51.36	67.54	83.65	51.43			
47	68	69.45	85.78	53.11	69.70	86.06	53.34			
48	71	72.54	89.24	55.85	72.61	89.31	55.91			
49	74	75.55	92.58	58.51	75.50	92.53	58.47			

Table A4. 95% Prediction confidence interval of software reliability models from 90% of Dataset 1.

Time	Real	GO			DS			YID		
		Prediction	Upper	Lower	Prediction	Upper	Lower	Prediction	Upper	Lower
45	65	58.35	73.32	43.38	65.02	80.82	49.21	66.13	82.07	50.19
46	66	59.64	74.78	44.50	66.73	82.74	50.72	68.13	84.31	51.96
47	68	60.93	76.23	45.63	68.42	84.63	52.21	70.15	86.56	53.73
48	71	62.22	77.68	46.76	70.10	86.51	53.69	72.17	88.82	55.52
49	74	63.51	79.14	47.89	71.76	88.36	55.16	74.19	91.08	57.31
Time	Real	PNZ			PZ			TP		
		Prediction	Upper	Lower	Prediction	Upper	Lower	Prediction	Upper	Lower
45	65	68.29	84.49	52.10	89.44	107.98	70.90	35.16	46.78	23.54
46	66	69.86	86.25	53.48	90.03	108.62	71.43	36.28	48.09	24.48
47	68	71.38	87.94	54.82	90.57	109.23	71.92	37.40	49.39	25.41
48	71	72.85	89.58	56.12	91.08	109.79	72.38	38.51	50.67	26.35
49	74	74.27	91.16	57.38	91.55	110.31	72.80	39.61	51.95	27.28
Time	Real	TC			Vtub			DPF		
		Prediction	Upper	Lower	Prediction	Upper	Lower	Prediction	Upper	Lower
45	65	65.76	81.65	49.86	65.89	81.80	49.98	63.71	79.35	48.06
46	66	67.66	83.78	51.53	67.78	83.91	51.64	64.82	80.60	49.04
47	68	69.56	85.90	53.21	69.66	86.02	53.30	65.85	81.75	49.94
48	71	71.45	88.02	54.89	71.53	88.11	54.95	66.80	82.82	50.78
49	74	73.35	90.13	56.56	73.39	90.19	56.60	67.68	83.81	51.56
Time	Real	UDPF			DNN			RNN		
		Prediction	Upper	Lower	Prediction	Upper	Lower	Prediction	Upper	Lower
45	65	83.99	101.95	66.03	66.72	82.73	50.71	66.52	82.50	50.53
46	66	85.64	103.78	67.51	68.57	84.80	52.34	67.43	83.52	51.33
47	68	87.28	105.59	68.97	69.72	86.08	53.35	69.45	85.78	53.11
48	71	88.89	107.36	70.41	71.70	88.30	55.11	72.54	89.23	55.85
49	74	90.47	109.11	71.83	74.70	91.64	57.76	75.61	92.65	58.57

Table A5. 95% Prediction confidence interval of software reliability models from 80% of Dataset 2.

Time	Real	Prediction	LSTM			GRU			Prediction	Upper	Lower
			Upper	Lower	Prediction	Upper	Lower				
45	65	66.55	82.54	50.56	66.52	82.51	50.54				
46	66	67.46	83.56	51.37	67.45	83.55	51.36				
47	68	69.50	85.84	53.16	69.50	85.84	53.16				
48	71	72.57	89.27	55.87	72.61	89.31	55.91				
49	74	75.58	92.62	58.54	75.69	92.74	58.64				
104	221	162.41	187.39	137.43	210.86	239.32	182.40	212.33	240.89	183.77	
105	227	163.96	189.06	138.87	214.68	243.40	185.96	216.29	245.12	187.47	
106	230	165.52	190.73	140.30	218.53	247.50	189.55	220.29	249.38	191.20	
107	242	167.07	192.40	141.74	222.40	251.63	193.17	224.32	253.67	194.96	
108	248	168.62	194.07	143.17	226.31	255.79	196.82	228.38	258.00	198.76	
109	261	170.18	195.74	144.61	230.24	259.98	200.50	232.48	262.36	202.60	
110	269	171.73	197.41	146.04	234.21	264.20	204.21	236.61	266.76	206.47	
111	279	173.28	199.08	147.48	238.20	268.45	207.95	240.78	271.20	210.37	
112	284	174.83	200.75	148.92	242.22	272.73	211.72	244.99	275.67	214.31	
113	287	176.38	202.41	150.35	246.27	277.03	215.52	249.23	280.17	218.28	
114	298	177.94	204.08	151.79	250.35	281.37	219.34	253.50	284.71	222.29	
115	313	179.49	205.75	153.23	254.46	285.73	223.20	257.81	289.28	226.34	
116	325	181.04	207.41	154.67	258.60	290.12	227.08	262.15	293.88	230.41	
117	335	182.59	209.08	156.11	262.76	294.53	230.99	266.53	298.52	234.53	
118	350	184.14	210.74	157.54	266.96	298.98	234.93	270.94	303.20	238.68	
119	366	185.69	212.40	158.98	271.18	303.45	238.90	275.38	307.91	242.86	
120	378	187.24	214.06	160.42	275.42	307.95	242.90	279.86	312.65	247.07	
121	386	188.79	215.73	161.86	279.70	312.48	246.92	284.38	317.43	251.33	
122	398	190.35	217.39	163.30	284.00	317.03	250.97	288.93	322.24	255.61	
123	406	191.90	219.05	164.74	288.34	321.62	255.05	293.51	327.09	259.93	
124	412	193.45	220.71	166.19	292.69	326.23	259.16	298.13	331.97	264.28	
125	422	195.00	222.37	167.63	297.08	330.86	263.30	302.78	336.88	268.67	
126	432	196.55	224.02	169.07	301.49	335.53	267.46	307.46	341.83	273.10	
127	449	198.10	225.68	170.51	305.93	340.22	271.65	312.18	346.81	277.55	
128	455	199.65	227.34	171.95	310.40	344.93	275.87	316.94	351.83	282.04	
129	476	201.19	229.00	173.39	314.90	349.68	280.11	321.73	356.88	286.57	

Time	Real	Prediction	PNZ		Prediction	PZ		Prediction	TP	
			Upper	Lower		Upper	Lower		Upper	Lower
104	221	487.7756	531.063	444.488	215.524	244.299	186.750	54.79	69.30	40.28
105	227	495.2823	538.902	451.663	219.663	248.712	190.614	55.61	70.23	40.99
106	230	502.8471	546.799	458.896	223.824	253.147	194.501	56.43	71.16	41.71
107	242	510.4698	554.753	466.186	228.005	257.600	198.409	57.26	72.10	42.43
108	248	518.1506	562.766	473.535	232.205	262.072	202.338	58.10	73.04	43.16
109	261	525.8893	570.837	480.942	236.421	266.558	206.284	58.94	73.99	43.90
110	269	533.6859	578.965	488.407	240.654	271.059	210.248	59.79	74.95	44.64
111	279	541.5405	587.152	495.929	244.900	275.572	214.227	60.65	75.91	45.38
112	284	549.4528	595.396	503.510	249.157	280.095	218.219	61.51	76.88	46.14
113	287	557.423	603.698	511.148	253.425	284.627	222.223	62.38	77.86	46.90
114	298	565.4509	612.058	518.844	257.701	289.165	226.237	63.25	78.84	47.67
115	313	573.5364	620.476	526.597	261.983	293.708	230.259	64.14	79.83	48.44
116	325	581.6795	628.951	534.408	266.270	298.253	234.288	65.03	80.83	49.22
117	335	589.88	637.483	542.277	270.560	302.800	238.321	65.92	81.84	50.01
118	350	598.138	646.073	550.203	274.851	307.345	242.356	66.82	82.85	50.80
119	366	606.4533	654.721	558.186	279.140	311.887	246.393	67.73	83.87	51.60
120	378	614.8259	663.425	566.226	283.427	316.424	250.430	68.65	84.89	52.41
121	386	623.2555	672.187	574.324	287.709	320.954	254.463	69.57	85.92	53.23
122	398	631.7421	681.006	582.479	291.984	325.476	258.493	70.51	86.96	54.05
123	406	640.2856	689.881	590.690	296.251	329.987	262.516	71.44	88.01	54.88
124	412	648.8858	698.813	598.958	300.508	334.485	266.531	72.39	89.06	55.71
125	422	657.5427	707.802	607.283	304.753	338.969	270.537	73.34	90.13	56.56

Table A5. Cont.

Time	Real	PNZ			PZ			TP		
		Prediction	Upper	Lower	Prediction	Upper	Lower	Prediction	Upper	Lower
126	432	666.256	716.847	615.665	308.985	343.437	274.532	74.30	91.20	57.41
127	449	675.0257	725.949	624.102	313.200	347.888	278.513	75.27	92.27	58.26
128	455	683.8516	735.107	632.596	317.399	352.318	282.480	76.24	93.36	59.13
129	476	692.7334	744.320	641.147	321.579	356.727	286.431	77.23	94.45	60.00
Time	Real	TC			Vtub			DPF		
		Prediction	Upper	Lower	Prediction	Upper	Lower	Prediction	Upper	Lower
104	221	212.53	241.10	183.96	215.13	243.88	186.38	210.95	239.42	182.48
105	227	216.44	245.27	187.60	219.32	248.34	190.29	214.13	242.82	185.45
106	230	220.38	249.48	191.28	223.54	252.85	194.24	217.27	246.16	188.38
107	242	224.35	253.71	194.99	227.80	257.39	198.22	220.36	249.46	191.27
108	248	228.35	257.97	198.73	232.10	261.97	202.24	223.41	252.70	194.11
109	261	232.38	262.26	202.50	236.44	266.58	206.30	226.40	255.89	196.91
110	269	236.44	266.58	206.30	240.82	271.23	210.40	229.34	259.02	199.66
111	279	240.53	270.93	210.13	245.23	275.92	214.53	232.23	262.09	202.36
112	284	244.65	275.31	213.99	249.67	280.64	218.70	235.06	265.11	205.01
113	287	248.80	279.71	217.88	254.16	285.40	222.91	237.83	268.06	207.61
114	298	252.97	284.15	221.80	258.67	290.20	227.15	240.55	270.95	210.15
115	313	257.18	288.61	225.75	263.23	295.03	231.43	243.21	273.78	212.65
116	325	261.41	293.10	229.72	267.81	299.89	235.74	245.81	276.54	215.09
117	335	265.68	297.62	233.73	272.44	304.79	240.09	248.36	279.25	217.47
118	350	269.97	302.17	237.76	277.09	309.72	244.47	250.84	281.89	219.80
119	366	274.29	306.75	241.82	281.78	314.68	248.88	253.27	284.46	222.08
120	378	278.63	311.35	245.91	286.51	319.68	253.33	255.63	286.97	224.30
121	386	283.01	315.98	250.03	291.26	324.71	257.81	257.94	289.42	226.46
122	398	287.41	320.64	254.18	296.05	329.78	262.33	260.19	291.80	228.57
123	406	291.84	325.32	258.35	300.87	334.87	266.87	262.37	294.12	230.63
124	412	296.29	330.03	262.55	305.72	340.00	271.45	264.50	296.38	232.63
125	422	300.77	334.77	266.78	310.61	345.15	276.07	266.57	298.57	234.57
126	432	305.28	339.53	271.04	315.52	350.34	280.71	268.58	300.70	236.46
127	449	309.82	344.32	275.32	320.47	355.56	285.38	270.54	302.77	238.30
128	455	314.38	349.13	279.63	325.44	360.80	290.09	272.43	304.78	240.08
129	476	318.97	353.97	283.96	330.45	366.08	294.82	274.27	306.73	241.81
Time	Real	UDPF			DNN			RNN		
		Prediction	Upper	Lower	Prediction	Upper	Lower	Prediction	Upper	Lower
104	221	207.30	235.52	179.08	224.90	254.29	195.51	223.38	252.67	194.09
105	227	210.58	239.02	182.13	231.12	260.92	201.32	229.02	258.68	199.36
106	230	213.86	242.52	185.20	232.86	262.76	202.95	233.04	262.96	203.12
107	242	217.14	246.02	188.26	245.66	276.38	214.94	243.36	273.94	212.78
108	248	220.43	249.53	191.33	252.12	283.24	221.00	249.67	280.64	218.70
109	261	223.72	253.03	194.40	264.58	296.46	232.70	262.29	294.03	230.54
110	269	227.01	256.54	197.48	272.98	305.36	240.59	270.43	302.66	238.20
111	279	230.30	260.05	200.56	282.82	315.78	249.86	280.34	313.16	247.52
112	284	233.60	263.55	203.64	288.04	321.30	254.77	285.86	319.00	252.72
113	287	236.89	267.06	206.73	289.86	323.22	256.49	289.90	323.27	256.53
114	298	240.19	270.56	209.81	301.74	335.79	267.69	299.40	333.31	265.48
115	313	243.48	274.07	212.90	316.42	351.28	281.55	314.27	349.02	279.52
116	325	246.78	277.57	215.99	328.66	364.19	293.13	326.29	361.70	290.89
117	335	250.08	281.07	219.08	338.82	374.90	302.74	336.33	372.28	300.39
118	350	253.37	284.57	222.17	353.42	390.27	316.57	351.27	388.01	314.54
119	366	256.67	288.07	225.27	369.34	407.00	331.67	367.27	404.83	329.71
120	378	259.96	291.56	228.36	381.66	419.95	343.37	379.29	417.46	341.12
121	386	263.25	295.06	231.45	389.98	428.68	351.27	387.43	426.01	348.85
122	398	266.54	298.54	234.55	401.66	440.94	362.38	399.30	438.46	360.13
123	406	269.83	302.03	237.64	409.98	449.66	370.29	407.43	446.99	367.87

Table A5. Cont.

Time	Real	UDPF			DNN			RNN		
		Prediction	Upper	Lower	Prediction	Upper	Lower	Prediction	Upper	Lower
124	412	273.12	305.51	240.73	416.12	456.10	376.14	413.69	453.55	373.82
125	422	276.41	308.99	243.82	425.82	466.27	385.37	423.36	463.68	383.03
126	432	279.69	312.47	246.91	435.82	476.74	394.90	433.34	474.14	392.54
127	449	282.97	315.94	250.00	452.26	493.94	410.57	450.27	491.86	408.68
128	455	286.24	319.40	253.08	459.12	501.12	417.12	456.64	498.53	414.76
129	476	289.52	322.86	256.17	478.93	521.83	436.04	477.26	520.08	434.44
Time	Real	LSTM			GRU					
		Prediction	Upper	Lower	Prediction	Upper	Lower			
104	221	224.52	253.89	195.15	224.46	253.82	195.09			
105	227	230.52	260.27	200.76	230.47	260.23	200.72			
106	230	233.63	263.59	203.67	233.09	263.02	203.17			
107	242	245.44	276.14	214.73	245.49	276.20	214.78			
108	248	251.49	282.58	220.41	251.49	282.58	220.41			
109	261	264.28	296.14	232.42	264.73	296.62	232.84			
110	269	272.32	304.67	239.98	272.77	305.14	240.40			
111	279	282.19	315.11	249.26	282.79	315.75	249.83			
112	284	287.44	320.67	254.21	287.72	320.96	254.47			
113	287	290.57	323.98	257.16	290.25	323.64	256.86			
114	298	301.38	335.41	267.36	301.60	335.64	267.56			
115	313	316.31	351.17	281.46	316.73	351.62	281.85			
116	325	328.25	363.76	292.74	328.79	364.33	293.25			
117	335	338.21	374.25	302.16	338.78	374.85	302.70			
118	350	353.18	390.02	316.35	353.75	390.62	316.89			
119	366	369.30	406.97	331.64	369.74	407.43	332.05			
120	378	381.25	419.52	342.98	381.69	419.98	343.40			
121	386	389.30	427.97	350.63	389.72	428.41	351.02			
122	398	401.13	440.39	361.88	401.67	440.96	362.39			
123	406	409.25	448.90	369.60	409.70	449.38	370.03			
124	412	415.37	455.31	375.42	415.78	455.75	375.82			
125	422	425.18	465.59	384.76	425.76	466.20	385.32			
126	432	435.14	476.03	394.26	435.72	476.64	394.81			
127	449	452.25	493.93	410.56	452.72	494.43	411.02			
128	455	458.45	500.42	416.49	458.79	500.77	416.81			
129	476	479.47	522.38	436.55	479.79	522.72	436.86			

Table A6. 95% Prediction confidence interval of software reliability models from 90% of Dataset 2.

Time	Real	GO			DS			YID		
		Prediction	Upper	Lower	Prediction	Upper	Lower	Prediction	Upper	Lower
117	335	215.85	244.65	187.06	284.80	317.88	251.73	285.07	318.16	251.98
118	350	217.69	246.61	188.77	289.52	322.87	256.17	289.81	323.18	256.45
119	366	219.53	248.57	190.49	294.27	327.89	260.65	294.59	328.24	260.95
120	378	221.37	250.53	192.21	299.06	332.95	265.16	299.41	333.33	265.50
121	386	223.21	252.49	193.93	303.88	338.05	269.71	304.26	338.45	270.08
122	398	225.05	254.45	195.65	308.74	343.18	274.30	309.16	343.62	274.69
123	406	226.89	256.41	197.37	313.63	348.34	278.92	314.08	348.82	279.35
124	412	228.73	258.37	199.08	318.56	353.54	283.58	319.05	354.05	284.04
125	422	230.57	260.33	200.80	323.52	358.78	288.27	324.05	359.33	288.76
126	432	232.40	262.28	202.53	328.52	364.05	293.00	329.08	364.64	293.53
127	449	234.24	264.24	204.25	333.56	369.35	297.76	334.16	369.98	298.33
128	455	236.08	266.20	205.97	338.63	374.69	302.56	339.27	375.37	303.16
129	476	237.92	268.15	207.69	343.73	380.07	307.39	344.41	380.79	308.04

Table A6. Cont.

Time	Real	PNZ			PZ			TP		
		Prediction	Upper	Lower	Prediction	Upper	Lower	Prediction	Upper	Lower
117	335	637.8859	687.388	588.383	312.9409	347.614	178.36	74.02	90.88	57.15
118	350	648.5408	698.455	598.627	320.3052	355.383	179.16	74.99	91.96	58.01
119	366	659.313	709.640	608.986	327.825	363.313	179.95	75.97	93.05	58.88
120	378	670.2031	720.944	619.462	335.505	371.406	180.74	76.95	94.14	59.76
121	386	681.2118	732.368	630.056	343.347	379.665	181.51	77.94	95.24	60.64
122	398	692.3398	743.912	640.768	351.355	388.094	182.28	78.94	96.35	61.52
123	406	703.5877	755.577	651.598	359.532	396.697	183.04	79.94	97.47	62.42
124	412	714.956	767.364	662.548	367.883	405.476	183.79	80.95	98.59	63.32
125	422	726.4455	779.273	673.618	376.411	414.437	184.54	81.97	99.72	64.23
126	432	738.0568	791.305	684.809	385.119	423.582	185.27	83.00	100.85	65.14
127	449	749.7904	803.460	696.121	394.011	432.916	186.00	84.03	101.99	66.06
128	455	761.647	815.739	707.555	403.091	442.443	186.72	85.07	103.14	66.99
129	476	773.6271	828.143	719.111	412.364	452.165	187.43	86.11	104.30	67.92
Time	Real	TC			Vtub			DPF		
		Prediction	Upper	Lower	Prediction	Upper	Lower	Prediction	Upper	Lower
117	335	300.84	334.83	266.84	315.55	350.37	280.74	314.95	349.74	280.17
118	350	306.57	340.89	272.26	322.66	357.87	287.45	322.44	357.63	287.24
119	366	312.37	347.01	277.73	329.85	365.45	294.25	330.07	365.68	294.46
120	378	318.23	353.20	283.27	337.12	373.10	301.13	337.86	373.89	301.83
121	386	324.15	359.44	288.86	344.46	380.84	308.09	345.80	382.25	309.35
122	398	330.13	365.74	294.51	351.88	388.65	315.12	353.90	390.77	317.03
123	406	336.16	372.10	300.23	359.37	396.53	322.22	362.16	399.46	324.86
124	412	342.26	378.52	306.00	366.93	404.48	329.39	370.58	408.31	332.85
125	422	348.42	385.00	311.83	374.56	412.49	336.63	379.17	417.33	341.00
126	432	354.63	391.54	317.72	382.25	420.57	343.93	387.92	426.52	349.31
127	449	360.91	398.14	323.67	389.99	428.70	351.29	396.83	435.88	357.79
128	455	367.25	404.81	329.69	397.79	436.89	358.70	405.92	445.41	366.43
129	476	373.64	411.53	335.76	405.65	445.12	366.17	415.18	455.12	375.25
Time	Real	UDPF			DNN			RNN		
		Prediction	Upper	Lower	Prediction	Upper	Lower	Prediction	Upper	Lower
117	335	313.06	347.74	278.38	342.30	378.56	306.04	344.31	380.68	307.94
118	350	319.88	354.94	284.83	357.85	394.93	320.77	359.54	396.70	322.38
119	366	326.81	362.24	291.37	373.93	411.83	336.03	375.59	413.58	337.61
120	378	333.83	369.64	298.02	385.60	424.09	347.11	387.48	426.06	348.90
121	386	340.96	377.15	304.77	392.86	431.70	354.01	395.19	434.15	356.22
122	398	348.19	384.77	311.62	405.60	445.08	366.13	407.38	446.94	367.82
123	406	355.53	392.49	318.57	412.86	452.68	373.03	415.14	455.07	375.20
124	412	362.97	400.31	325.63	417.20	457.23	377.16	420.72	460.92	380.52
125	422	370.52	408.25	332.79	429.30	469.91	388.69	431.01	471.71	390.32
126	432	378.17	416.29	340.06	439.30	480.38	398.22	441.16	482.33	400.00
127	449	385.93	424.44	347.43	457.00	498.90	415.10	458.57	500.55	416.60
128	455	393.80	432.70	354.91	460.20	502.24	418.15	464.02	506.24	421.80
129	476	401.78	441.06	362.49	484.30	527.43	441.17	485.63	528.82	442.44
Time	Real	LSTM			GRU					
		Prediction	Upper	Lower	Prediction	Upper	Lower			
117	335	344.69	381.08	308.30	341.00	377.20	304.81			
118	350	359.89	397.08	322.71	356.47	393.48	319.47			
119	366	376.04	414.05	338.04	372.84	410.68	334.99			
120	378	388.18	426.80	349.56	384.75	423.19	346.30			
121	386	396.10	435.10	357.09	392.09	430.91	353.28			
122	398	408.02	447.61	368.43	404.27	443.68	364.86			
123	406	415.90	455.87	375.93	411.73	451.50	371.95			
124	412	421.43	461.67	381.20	416.92	456.94	376.90			
125	422	431.44	472.15	390.73	427.32	467.83	386.80			

Table A6. Cont.

Time	Real	Prediction	LSTM		Prediction	GRU	
			Upper	Lower		Upper	Lower
126	432	441.49	482.67	400.31	437.55	478.54	396.55
127	449	458.83	500.81	416.85	455.32	497.14	413.50
128	455	464.67	506.92	422.42	460.27	502.32	418.22
129	476	485.82	529.02	442.62	482.13	525.17	439.09

References

- Jelinski, Z.; Moranda, P. Software reliability research. In *Statistical Computer Performance Evaluation*; Elsevier: Amsterdam, The Netherlands, 1972; pp. 465–484.
- Goel, A.L.; Okumoto, K. Time-dependent error-detection rate model for software reliability and other performance measures. *IEEE Trans. Reliab.* **1979**, *28*, 206–211. [[CrossRef](#)]
- Yamada, S.; Ohba, M.; Osaki, S. S-shaped reliability growth modeling for software error detection. *IEEE Trans. Reliab.* **1983**, *32*, 475–484. [[CrossRef](#)]
- Ohba, M. Inflection S-shaped software reliability growth model. In *Stochastic Models in Reliability Theory*; Osaki, S., Hatoyama, Y., Eds.; Springer: Berlin, Germany, 1984; pp. 144–162.
- Zhang, X.M.; Teng, X.L.; Pham, H. Considering fault removal efficiency in software reliability assessment. *IEEE Trans. Syst. Man. Cybern. Part Syst. Hum.* **2003**, *33*, 114–120. [[CrossRef](#)]
- Yamada, S.; Tokuno, K.; Osaki, S. Imperfect debugging models with fault introduction rate for software reliability assessment. *Int. J. Syst. Sci.* **1992**, *23*, 2241–2252. [[CrossRef](#)]
- Pham, H.; Zhang, X. An NHPP software reliability models and its comparison. *Int. J. Reliab. Qual. Saf. Eng.* **1997**, *4*, 269–282. [[CrossRef](#)]
- Pham, H.; Nordmann, L.; Zhang, X. A general imperfect software debugging model with S-shaped fault detection rate. *IEEE Trans. Reliab.* **1999**, *48*, 169–175. [[CrossRef](#)]
- Teng, X.; Pham, H. A new methodology for predicting software reliability in the random field environments. *IEEE Trans. Reliab.* **2006**, *55*, 458–468. [[CrossRef](#)]
- Kapur, P.K.; Pham, H.; Anand, S.; Yadav, K. A unified approach for developing software reliability growth models in the presence of imperfect debugging and error generation. *IEEE Trans. Reliab.* **2011**, *60*, 331–340. [[CrossRef](#)]
- Roy, P.; Mahapatra, G.S.; Dey, K.N. An NHPP software reliability growth model with imperfect debugging and error generation. *Int. J. Reliab. Qual. Saf. Eng.* **2014**, *21*, 1450008. [[CrossRef](#)]
- Chang, I.H.; Pham, H.; Lee, S.W.; Song, K.Y. A testing-coverage software reliability model with the uncertainty of operation environments. *Int. J. Syst. Sci. Oper. Logist.* **2014**, *1*, 220–227. [[CrossRef](#)]
- Pham, H. A new software reliability model with Vtub-Shaped fault detection rate and the uncertainty of operating environments. *Optimization* **2014**, *63*, 1481–1490. [[CrossRef](#)]
- Pham, L.; Pham, H. Software reliability models with time-dependent hazard function based on bayesian approach. *IEEE Trans. Syst. Man, Cybern.-Part A Syst. Humans* **2000**, *30*, 25–35. [[CrossRef](#)]
- Kim, Y.S.; Song, K.Y.; Pham, H.; Chang, I.H. A software reliability model with dependent failure and optimal release time. *Symmetry* **2022**, *14*, 343. [[CrossRef](#)]
- Lee, D.H.; Chang, I.H.; Pham, H. Software reliability growth model with dependent failures and uncertain operating environments. *Appl. Sci.* **2022**, *12*, 12383. [[CrossRef](#)]
- Kim, Y.S.; Chang, I.H.; Lee, D.H. Non-parametric software reliability model using deep neural network and NHPP software reliability growth model comparison. *J. Korean Data Anal. Soc.* **2020**, *22*, 2371–2382. [[CrossRef](#)]
- Miyamoto, S.; Tamura, Y.; Yamada, S. Reliability assessment tool based on deep learning and data preprocessing for OSS. *Am. J. Oper. Res.* **2022**, *12*, 111–125. [[CrossRef](#)]
- Wang, J.; Zhang, C. Software reliability prediction using a deep learning model based on the RNN encoder–decoder. *Reliab. Eng. Syst. Saf.* **2018**, *170*, 73–82. [[CrossRef](#)]
- Oveisi, S.; Moeini, A.; Mirzaei, S. LSTM encoder-decoder dropout model in software reliability prediction. *Int. J. Reliab. Risk Saf. Theory Appl.* **2021**, *4*, 1–12. [[CrossRef](#)]
- Raamesh, L.; Jothi, S.; Radhika, S. Enhancing software reliability and fault detection using hybrid brainstorm optimization-based LSTM model. *IETE J. Res.* **2022**, 1–15. [[CrossRef](#)]
- Karunanithi, N.; Whitley, D.; Malaiya, Y.K. Using neural networks in reliability prediction. *IEEE Softw.* **1992**, *9*, 53–59. [[CrossRef](#)]
- Singh, Y.; Kumar, P. Prediction of software reliability using feed forward neural networks. In *Proceedings of the 2010 International Conference on Computational Intelligence and Software Engineering*, Wuhan, China, 10–12 December 2010; pp. 1–5.
- Graves, A. Generating sequences with recurrent neural networks. *arXiv* **2013**, arXiv:1308.0850.
- Bengio, Y.; Simard, P.; Frasconi, P. Learning long-term dependencies with gradient descent is difficult. *IEEE Trans. Neural Netw.* **1994**, *5*, 157–166. [[CrossRef](#)] [[PubMed](#)]

26. Jozefowicz, R.; Zaremba, W.; Sutskever, I. An empirical exploration of recurrent network architectures In Proceedings of the 32nd International Conference on Machine Learning (ICML-15), Lille, France, 6–11 July 2015.
27. Gers, F.A.; Schmidhuber, J.; Cummins, F. Learning to forget: Continual prediction with LSTM. *Neural Comput.* **2000**, *12*, 2451–2471. [[CrossRef](#)]
28. Inoue, S.; Yamada, S. Discrete software reliability assessment with discretized NHPP models. *Comput. Math. Appl.* **2006**, *51*, 161–170. [[CrossRef](#)]
29. Askari, R.; Sebt, M.V.; Amjadian, A. A multi-product EPQ model for defective production and inspection with single machine, and operational constraints: Stochastic programming approach. *Commun. Comput. Infor. Sci.* **2021**, *1458*, 161–193.
30. Jeske, D.R.; Zhang, X. Some successful approaches to software reliability modeling in industry. *J. Syst. Softw.* **2005**, *74*, 85–99. [[CrossRef](#)]
31. Iqbal, J. Software reliability growth models: A comparison of linear and exponential fault content functions for study of imperfect debugging situations. *Cogent Eng.* **2017**, *4*, 1286739. [[CrossRef](#)]
32. Pillai, K.; Sukumaran Nair, V.S. A model for software development effort and cost estimation. *IEEE Trans. Softw. Eng.* **1997**, *23*, 485–497. [[CrossRef](#)]
33. Souza, R.L.C.; Ghasemi, A.; Saif, A.; Gharaei, A. Robust job-shop scheduling under deterministic and stochastic unavailability constraints due to preventive and corrective maintenance. *Comput. Ind. Eng.* **2022**, *168*, 108130. [[CrossRef](#)]
34. Li, Q.; Pham, H. NHPP software reliability model considering the uncertainty of operating environments with imperfect debugging and testing coverage. *Appl. Math. Model.* **2017**, *51*, 68–85. [[CrossRef](#)]
35. Pham, H. *System Software Reliability*; Springer: London, UK, 2006.

Disclaimer/Publisher’s Note: The statements, opinions and data contained in all publications are solely those of the individual author(s) and contributor(s) and not of MDPI and/or the editor(s). MDPI and/or the editor(s) disclaim responsibility for any injury to people or property resulting from any ideas, methods, instructions or products referred to in the content.